Potentiodynamic electrochemical impedance spectroscopy of lead upd on polycrystalline gold and on selenium atomic underlayer

A.S. Bondarenko, G.A. Ragoisha[*], N.P. Osipovich, E.A. Streltsov

Belarusian State University, 220050 Minsk, Belarus

Abstract

Pb upd on polycrystalline Au and on Au coated with Se atomic layer was investigated by potentiodynamic electrochemical impedance spectroscopy. Faradaic and double layer responses have disclosed two distinct stages in Pb upd on Au: a partly irreversible stage, attributed to formation and growth of Pb 2D islands, and a reversible phase transition in the final stage of a monolayer deposition. The completion of a continuous monolayer formation in the potential scan was signalised by a sharp minimum in double layer pseudocapacitance Q_{dl}. Pb^{2+} reduction, which was monitored concurrently by parameters of Faradaic response, continued shortly after the Q_{dl} minimum and showed sharp maxima of adsorption capacitance and inverse Warburg constant at 40 mV below Q_{dl} minimum. This was explained by surface free energy minimisation that forced continuous atomic layer formation with inclusion of some lead cations into Pb monolayer. The two-stage Pb upd transformed into a single-stage strongly irreversible upd as a result of Se atomic underlayer deposition on Au.

1. Upd investigation by PDEIS

Potentiodynamic electrochemical impedance spectroscopy (PDEIS) [1-3] acquires and analyses electrochemical response of interface as functions of frequency and electrode potential. Simultaneous analysis of frequency and potential dependences enables separation of ac response components that originate from different processes and interfacial structures. The PDEIS spectrum analyser presents constituent responses by corresponding elements of equivalent electric circuits (EEC) as functions of the potential in a potential scan, and this enables individual monitoring of interrelated processes on nonstationary interfaces. To cope with the nonstationarity, PDEIS operates in a limited range of frequencies. Because of the limited frequency range, PDEIS monitors only those constituents that respond in the frequency range tested; in return, the additional variable (electrode potential) facilitates distinguishing of confusing circuits [1]. Unlike stationary EIS that strives for the widest frequency range to present a complete EEC of a stationary state, PDEIS concentrates on evolution of constituent responses in the range of overlapping double layer and Faradaic responses. The separation of the constituent potentiodynamic ac responses turns the double layer and Faradaic processes into efficient intrinsic interfacial probes [1, 3-6].

PDEIS appeared to be especially helpful for nonstationary effects monitoring in upd [1, 3-5]. Different equivalent circuits were found for reversible and irreversible upd. Low-amplitude ac probing of the reversible upd causes oscillation of adatom coverage, which produces the capacitance of adsorption in the EECs of Cu [3] and Bi [1] upd on Au. On the contrary, no adsorption capacitance was found in the irreversible Pb upd on Te [4], Ag upd on Pt [5], and Te upd on Au [6], where cathodic deposition of atomic layers and their anodic destruction did not overlap. Moreover, PDEIS enabled separate monitoring of anions coadsorption in Cu [3] and Bi [1] upd on Au and disclosed different paths for forward and backward processes in Cu and Bi monolayers formation and destruction in presence of complex oxygen-containing anions (sulphate, nitrate and perchlorate). Interestingly, small and symmetric chloride anions adsorbed perfectly reversibly in Cu upd on Au [7,8], though their adsorption produced complex dependences on potential of capacitances and resistances attributed to cation and anion adsorption. Pettit et al [9] have obtained recently the same equivalent circuit with separate RC branches for cations and anions in their study of Cu^{2+} and ClO_4^- mutually correlated adsorption with time resolved Fourier transform impedance spectroscopy. The EEC with separate RC branches for cation and anion adsorption was obtained also in stationary EIS in the investigation of hydrogen upd [10]. The observation of the two RC branches in Cu upd on Au by different research groups that used different dynamic EIS techniques [3,9] and the recurrence of the same equivalent circuit in Bi upd on Au [1] destroy the myth of fundamental

---
[*] Corresponding author. Tel./fax: +375-17-2264696.
E-mail address: ragoishag@bsu.by (Genady Ragoisha).

inseparability of cations and anions adsorption in upd. The constituent processes were inseparable in dc and single frequency ac responses, but PDEIS got the information from frequency response variation, which was specific for each constituent of the interfacial processes. The separation of cooperative processes is one of the most interesting new possibilities of dynamic frequency response analysis.

Investigations of atomic level processes on surfaces of monocrystals have become common with in situ probe microscopic techniques, however, STM and AFM are not very helpful in the case of polycrystalline and amorphous substrates, where intrinsic variations of relief exceed the variations that result from atomic layers deposition. Multi-parametric characterisation of electrochemical response by dynamic frequency response analysis makes no special demand of the surface relief and thus is especially promising for nonstationary processes monitoring on real complex surfaces.

This work presents PDEIS application for characterisation of reversible, though intrinsically complex, Pb upd on polycrystalline Au and the transformation of the reversible upd into irreversible upd by selenium atomic underlayer. Unlike Cu and Bi upd, which show complexities that result from coadsorbing anions, electrosorption of lead cations on gold is very complex in itself [11-28]. Pb upd was investigated on various crystal faces and polycrystalline Au with cyclic voltammetry and STM [11-32], however, the nature of two-humped voltammograms that split further into additional peaks is still the object of investigations and speculations [33-34]. The splitting is usually ascribed to kinetics of the process [33]: the peak at higher underpotential corresponds to the growth of the lead deposited island, whereas the one at lower underpotential corresponds to the coalescence process. First-order phase transition in 2D-phase was observed in the final stage of Pb upd on Au (100) [32]. A two-humped shape of the voltammogram of Pb upd on polycrystalline gold was explained also by thermodynamic reasons in the framework of Frumkin isotherm [34]. The thermodynamic approach in principle is applicable to different mechanisms; however, in the thermodynamic consideration presented in [34] adsorption sites of two types with different energies were presumed already in the initial stage of upd. That situation was physically different from what was considered in explanation of Pb upd complexity by phase transition and kinetic reasons. Both the phase transition and coalescence are cooperative phenomena that require certain preceding changes in the system (accumulation of islands or formation of a 2D phase capable of transforming to another, more dense 2D phase in the next stage of adatom deposition). Because of the complexity of Pb upd on Au, it was interesting to examine the possibilities of PDEIS for that system, in particular on polycrystalline electrodes inconvenient for investigation with scanning probe techniques.

The other goal of the PDEIS investigation of lead atomic layers was motivated by Pb upd application for multilayers and quantum confined PbSe nanoparticles assembling by electrochemical atomic layer epitaxy (ECALE) [35]. ECALE is a promising instrument for nanotechnology and it requires monitoring of the interface properties variation during the assembling. In our expectation muti-parametric characterisation based on PDEIS could be appropriate for this case. Pb upd on Se atomic layer is the first stage in the electrochemical assembling of PbSe quantum confined particles on Au, so it was interesting to compare dynamic frequency response of Pb upd on bare gold and on Au covered with Se atomic layer.

Experimental.

Au wire (ChemPur, 0.015 cm^2 geometric surface area) electrode was treated with nitrohydrochloric acid, rinsed, flame annealed, and after cycling in 0.1M $HClO_4$ for reproducible surface status placed into 1mM $Pb(ClO_4)_2$ + 0.1M $HClO_4$ aqueous solution for Pb deposition or into 1mM SeO_2 + 0.1M $HClO_4$ for Se deposition. Pb atomic layers were deposited onto bare polycrystalline gold and onto predeposited selenium atomic underlayer in potential scans from 0.30 V to -0.42 V (versus Ag|AgCl|KCl(sat) reference electrode) and stripped off in reverse scans with continuous recording of PDEIS spectra. The scan rate was 2 mV/s. PDEIS spectra were recorded and analysed as described in [1,2] in the frequency range from 17 Hz to 702 Hz. Typical PDEIS spectra of Pb upd on bare Au and on Au covered with Se atomic layer and also some examples of constant potential sections of the 3D spectra (Nyquist plots) are shown in Fig.1. Forward and backward scans give very similar PDEIS spectra on Au, except for initial stages of the upd, that show somewhat different responses in the cathodic and anodic scans. On the contrary, in the case with Se underlayer the spectrum in the anodic scan differs considerably from the spectrum recorded in the cathodic scan. The characteristic strong changes in the imaginary impedance, attributed to Pb atomic layer deposition and removal, in the latter case were observed at appreciably different potentials, due to irreversibility of Pb upd on Se atomic underlayer.
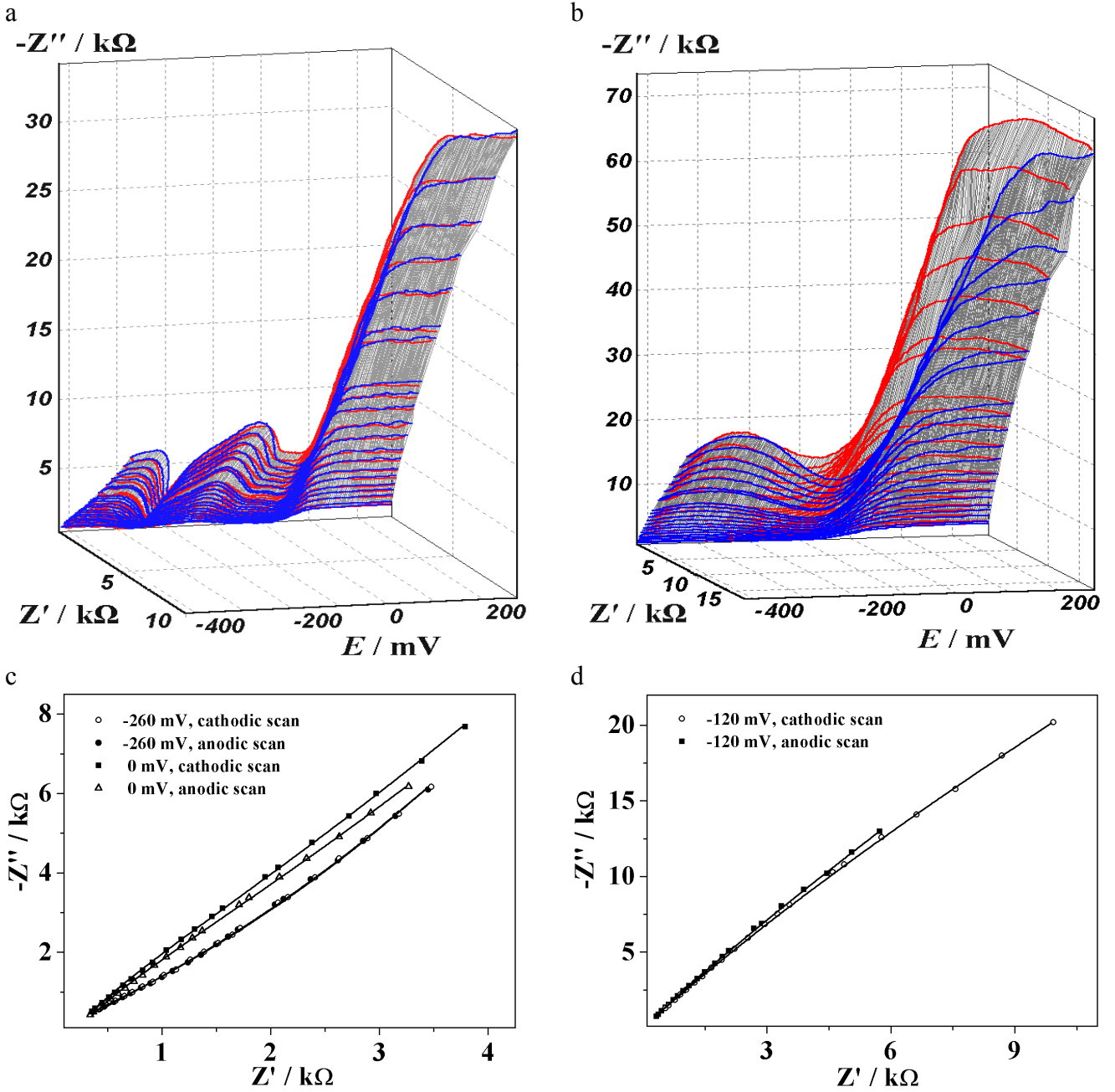
Fig. 1. Cyclic PDEIS spectra of (a) Pb upd on Au and (b) Pb upd on Au coated with selenium atomic layer; (c, d) examples of constant potential sections of PDEIS spectra for Pb upd on (c) bare Au and (d) Au coated with selenium atomic layer. Cathodic (red) and anodic (blue) scans in PDEIS spectra are presented in different colours in the electronic version. dE/dt = 2 mV/s. Solid lines in (c) and (d) show fit to corresponding equivalent circuits.

In Se atomic layer deposition, the cathodic scan from 0.8 V was stopped at 0.3 V to prevent nucleation of bulk Se that occurred at lower potentials [36-40]. Se deposition charge was 300 μC cm^{-2}, which should correspond to approximately 0.35 monolayer according to [40]. PDEIS spectrum for Se deposition in the potential range of Se atomic layer deposition, similarly to PDEIS spectra of irreversible upd of Pb on Te [4] and Ag on Pt [5], fitted well to a Randles type equivalent circuit with the double layer capacitance represented by constant phase element (Fig. 2a). The exponent n of the CPE impedance $Z_{cpe}=Q_{dl}^{-1}(j\omega)^{-n}$ was in the range between 0.94 and 1.0. Se atomic layer deposition was observed by more than a fivefold decrease in double layer pseudocapacitance Q_{dl} below 0.45 V in the cathodic scan. We would like to note that the EEC fit was examined both on the frequency and potential scales. Occasionally, in some of the constant potential sections more than one EEC fitted to the data with χ^2 below 10^{-4}, however, due to variation of contributions of different EEC elements with the variable potential, confusing circuits were easily excluded in the examination on the potential scale. The new opportunities based on 3D fit in PDEIS have been considered recently in [1].
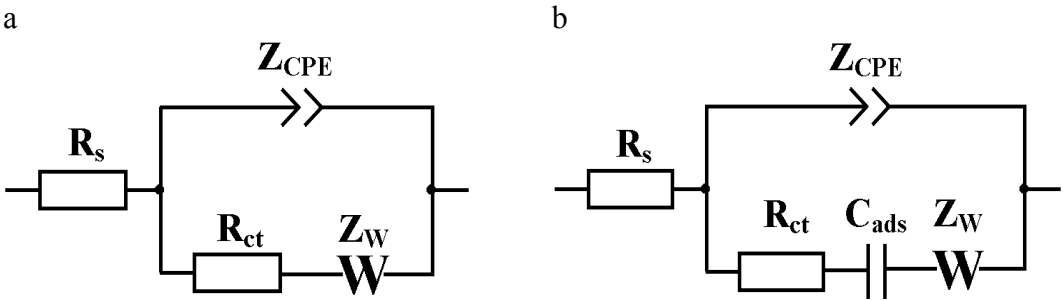
Fig. 2. The best fit equivalent electric circuits for the potentiodynamic frequency response of (a) Se atomic layer deposition on Au and Pb upd on Se atomic underlayer, (b) Pb upd on Au. Z_{CPE} is the impedance of a constant phase element, Z_W – impedance of Warburg element, R_{ct} – charge transfer resistance, C_{ads} – adsorption capacitance, R_S – resistance of electrolyte solution.
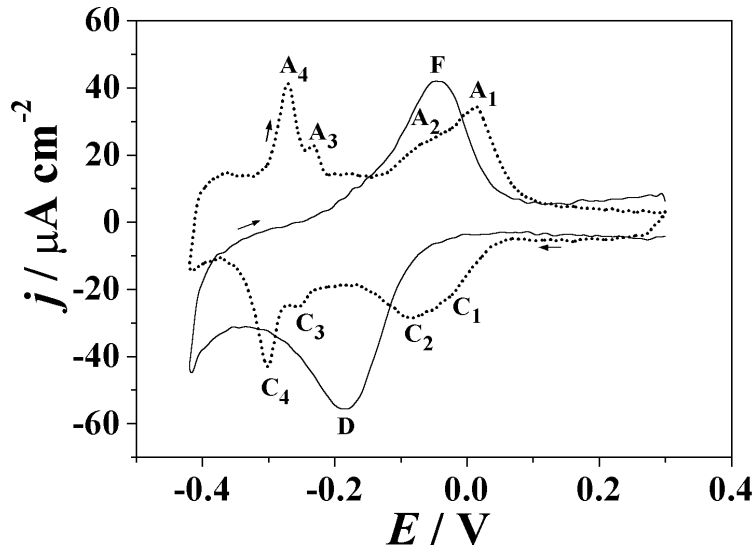
Fig. 3. Cyclic voltammograms of bare Au electrode (dotted) and Au electrode coated with selenium atomic layer (solid) in 1 mM $Pb(ClO_4)_2$ + 0.1 M $HClO_4$. dE/dt = 58 mV/s.

The PDEIS spectra analysis gave the EEC shown in Fig. 2b for Pb upd on Au. Additionally to the EEC of irreversible upd it contains adsorption capacitance, which is a signature of a reversible upd. Faradaic part of impedance in the frequency range tested was determined almost completely by the impedance of adsorption capacitance $Z_C=1/(j\omega C_{ads})$ and Warburg impedance $Z_W=A/(j\omega)^{0.5}$, where ω was circular frequency, j – imaginary unit, C_{ads} – adsorption capacitance, A – Warburg constant. Therefore, Faradaic impedance in Pb upd on Au was monitored by C_{ads} and A variations, while the changes in double layer were monitored by the variation of double layer pseudocapacitance. The CPE exponent in that case was between 0.96 and 1.0. Se atomic underlayer eliminated the adsorption capacitance, so that the EEC of Pb upd on Se underlayer appeared to be the same as for Se atomic layer deposition (Fig. 2a). The CPE exponent in Pb upd on Se underlayer was between 0.85 and 0.94.

Results and Discussion.

Fig. 3 shows cyclic voltammograms (CV) of lead upd on bare Au electrode and on Au electrode covered with atomic layer of selenium. Pb upd on Au starts below 0.05 V. Both the cathodic and anodic branches of the voltammogram show four peaks, cathodic $C_1 - C_4$ and anodic $A_1 - A_4$. The peaks A_1, A_2 are shifted positively from the corresponding cathodic peaks C_1, C_2 thus showing the irreversibility effects in the initial stage of Pb upd on Au. On the contrary, the peaks C_3, C_4, A_3, A_4 show good reversibility of the final stage of the upd. This behaviour is typical for Pb upd on Au [33].

a

b

c
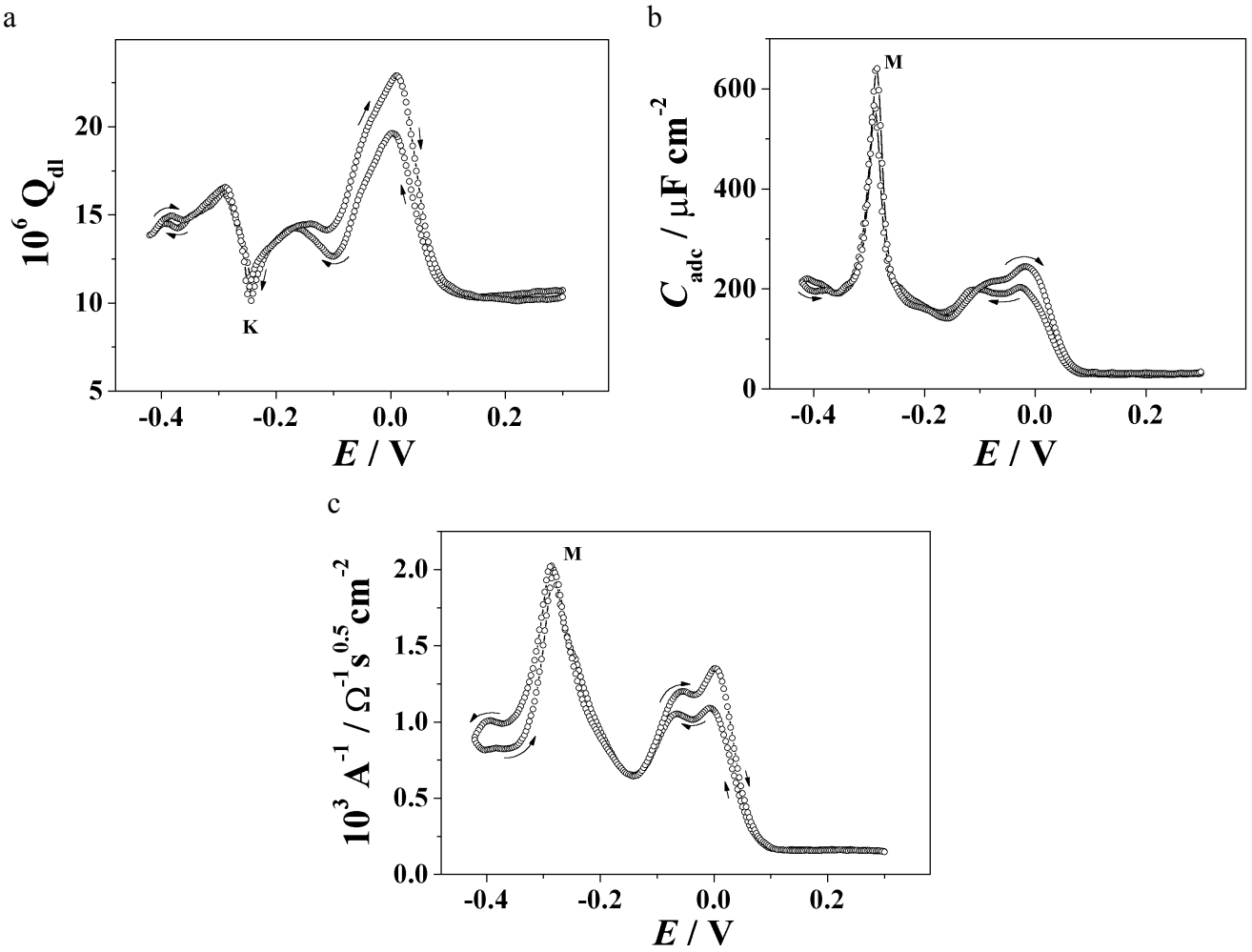
Fig. 4. EEC parameters variation in cyclic potential scan in Pb upd on Au: (a) double layer pseudocapacitance Q_{dl}, (b) adsorption capacitance C_{ads}, (c) inverse Warburg constant A^{-1}.
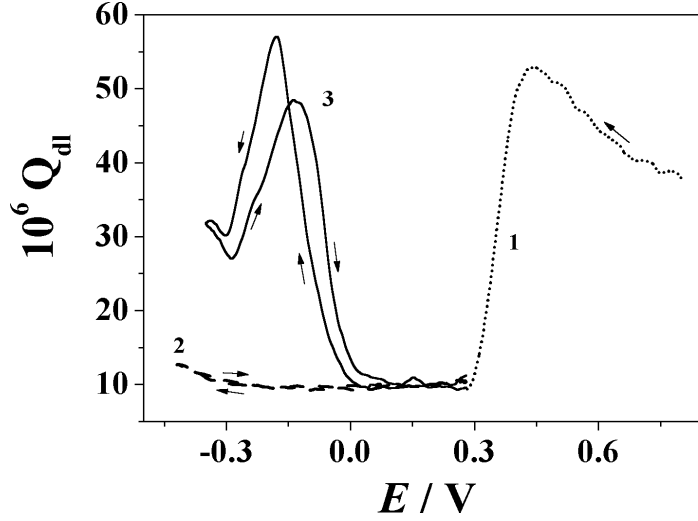
Fig. 5. Double layer pseudocapacitance Q_{dl} variation with the potential of Au electrode (1) and Au electrode coated with selenium atomic layer (2,3). Electrolytes: 1mM SeO_2 + 0.1M $HClO_4$ (1), 0.1M $HClO_4$ (2), 1mM $Pb(ClO_4)_2$ + 0.1M $HClO_4$ (3).

Fig. 4 shows the variation of the double layer pseudocapacitance, adsorption capacitance and inverse Warburg constant for Pb upd on Au in cyclic potential scan. All the three dependences, similarly to the CV, show partly irreversible and reversible stages of the upd, but the variation of equivalent circuit elements is more complex and contains more information than the CV. The analysis of the PDEIS spectrum has allowed separate monitoring of double layer pseudocapacitance and parameters of Faradaic

impedance that showed different signatures on the potential scale. In particular, the minimum K in Fig. 4a was observed at 40 mV above the maxima M in Figs. 4b,c. Thus, the maximum of the adsorption capacitance was achieved in the upd shortly after the minimum of the double layer pseudocapacitance.

Selenium atomic underlayer changes dramatically the upd of lead (Fig. 3). Pb upd on Se atomic layer started at lower underpotential than on gold and instead of the series of reversible and irreversible peaks only a pair of cathodic and anodic peaks (D and F) was observed. The anodic peak F shows a considerable positive shift from the cathodic peak D, which discloses the irreversible nature of Pb upd on atomic layer of Se. Background current observed by the end of the cathodic scan was probably due to hydrogen reduction. The catalytic effect of Pb on bulk Se in the same potential range was reported in [42].

Curve 1 in Fig. 5 shows a decrease in Q_{dl} during the deposition of Se atomic layer on Au in the cathodic scan from 0.8 to 0.3 V. At 0.3 V the external voltage was switched off, the electrode was rinsed with 0.1 M $HClO_4$ and placed into 0.1 M $HClO_4$. In the earlier work [36] Se atomic layer was found to remain intact in a similar procedure. Se atomic layer preservation in this work was verified by anodic stripping voltammetry. Upon the electrode transposition into 0.1 M $HClO_4$, the same potential (0.3 V) was applied and the potentiodynamic response was recorded in cyclic potential scan between 0.3 V and -0.4 V. Curve 2 in Fig. 5 shows that Q_{dl} remains almost constant in that scan. The electrode was transferred then into a new solution: 0.1 M $HClO_4$ + 0.001 M $Pb(ClO_4)_2$ and again a cyclic scan was recorded (curve 3 in Fig. 5). During Pb upd on Se atomic layer Q_{dl} passes a maximum and shows a considerable hysteresis in reverse scan. Q_{dl} variation shows the similar irreversibility of Pb upd on Se atomic layer as was observed in CV. A small increase in Q_{dl} below -0.3 V resulted obviously from the background hydrogen reduction that affected the interface status in that potential range.

Thus, both the CV and PDEIS show partly irreversible and reversible stages in Pb upd on Au and the transformation of the two-stage upd into a single irreversible process as a result of Se atomic layer deposition on Au.

The initiation of Pb 2D islands growth is determined by Au surface, while the reverse process is controlled by the parameters of Pb-Au system, therefore the initial stage of Pb upd on Au shows the deviation from reversibility both in Faradaic and double layer responses. The rise in Q_{dl} in the scan from 0.1 V to 0 V results mainly from Pb adatoms deposition. Below 0 V the growth of the islands probably dominates over the increase in their concentration. The observed Q_{dl} decrease may be due to decrease of unitary surface area specific capacity of the growing Pb atomic layer, and this may result from changes in orientation of water dipoles. The effect of Pb-H_2O interaction on capacity of Pb atomic layer formed by upd on Te was considered earlier [4]. Sharp minimum K obviously indicates the completion of a continuous Pb atomic layer formation.

We assume that the surface free energy minimisation during the continuous Pb atomic layer formation forces inclusion of some lead cations into the deposited atomic layer. Probably for this reason the peaks M in C_{ads} and A^{-1} variation in the cathodic scan (Figs. 4b and 4c) lag 40 mV behind the minimum K in Q_{dl}. Parameters of Faradaic response (C_{ads} and A^{-1}) relate to Pb^{2+} reduction, rather than the formation of the monolayer, and peaks M in Figs. 4b and 4c indicate the completion of Pb^{2+} reduction. Thus the range between K and M extrema corresponds to Pb^{2+} reduction in the continuous layer. The latter is formed abruptly around the potential of Q_{dl} minimum by a pseudo phase transition from less compactly distributed Pb adatoms. Final changes of the parameters below the potential of peak M probably result from the double layer restructuring on the newly formed interface.

The pseudo phase transition in the final stage of Pb monolayer deposition appears to be perfectly reversible, both in the Faradaic and double layer responses (Fig. 4). The reversibility of the final stage of Pb upd on Au discloses collective interactions in Pb atomic layer, which results from the delocalised and collective nature of Pb-Au metallic bond. Selenium underlayer hinders the collective behaviour of Pb atomic layer, due to more localised character of Pb-Se interaction. Interatomic interactions in Pb layer become less significant and therefore the potentiodynamic response in Pb upd on Se atomic layer shows only one extremum, both in CV (Fig.3) and PDEIS (Fig. 5). The covalent interaction determines also the irreversibility of Pb upd on Se atomic layer that shows up in CV and PDEIS. Similar irreversibility was observed in Pb upd on PbSe [41,42] and Pb upd on Te [4]. The localised interactions between Pb and Se atoms were used in the electrochemical synthesis of PbSe [41-45].

Conclusions

Pb upd on polycrystalline Au and on Se atomic underlayer on Au was investigated by potentiodynamic electrochemical impedance spectroscopy. The multivariate frequency response in PDEIS was decomposed into components related to Faradaic and double layer responses, which provided the individual constituent responses monitoring in the dynamic conditions of upd. The Faradaic and double layer responses in Pb upd on Au have shown two distinct stages: a partly irreversible first stage, attributed to the formation and growth of Pb 2D islands, and a reversible second stage, attributed to the formation of a compact Pb atomic layer. The latter stage manifested itself as a phase transition in the variation of constituent ac responses, and this was explained by strongly delocalised character of atomic interactions in Pb monolayer on Au. The localisation of Pb adatom interaction on Se atomic underlayer decreases the collective behaviour of Pb atomic layer, which results in the transformation of the complex two-stage process into a single-step strongly irreversible Pb upd on Se atomic underlayer. The EEC, correspondingly, changes to a simpler one (without adsorption capacitance). Thus, a bilayer assembling was for the first time examined with PDEIS and the results confirm the availability of this technique for monitoring of atomic layers assembling on complex nonideal surfaces.

References

1. G.A. Ragoisha, A.S. Bondarenko, Electrochim. Acta 50 (2005) 1553.
2. G.A. Ragoisha, A.S. Bondarenko, Solid State Phenom. 90-91 (2003) 103.
3. G.A. Ragoisha, A.S. Bondarenko, Electrochem. Commun. 5 (2003) 392.
4. G.A. Ragoisha, A.S. Bondarenko, N.P. Osipovich, E.A. Streltsov, J. Electroanal. Chem. 565 (2004) 227.
5. G.A. Ragoisha, A.S. Bondarenko, Surf. Sci. 566-568 (2004) 315.
6. G.A. Ragoisha, A.S. Bondarenko, Phys. Chem. Appl. Nanostructures, World Scientific, 2003, 373.
7. G.A. Ragoisha, A.S. Bondarenko, in: S.A. Maskevich, V.F. Stelmakh, A.K. Fedotov (Eds.), Low-Dimensional Systems – 2. Physical Chemistry of Elements and Systems with Low-Dimensional Structuring (in Russian), Grodno, 2004, 87.
8. G.A. Ragoisha, A.S. Bondarenko. In: Progress in Electrochemistry Research, Nova Science Publishers, NY, 2005 (in press, ISBN: 1-59454-449-2).
9. C.M. Pettit, J.E. Garland, M.J. Walters, D. Roy, Electrochim. Acta 49 (2004) 3293.
10. S. Morin, H. Dumont, B.E. Conway, J. Electroanal. Chem. 412 (1996) 39.
11. T. Takamura, K. Takamura, W. Nippe, E. Yeager, J. Electrochem. Soc. 117 (1970) 626.
12. E. Schmidt, N. Wüthrich, J.Electroanal. Chem. 34 (1972) 377.
13. V.A. Vicente, S. Bruckenstein, Anal.Chem. 45 (1973) 2036.
14. T. Takamura, F. Watanabe, K. Takamura, Electrochim. Acta. 19 (1974) 933.
15. B.E. Conway, H. Angerstein-Kozlovska, US Nat. Bur. Stand. Spec. Publ. 455 (1976) 107.
16. R. Adzic, E. Yeager, B.D. Cahan, J. Electrochem. Soc. 121 (1974) 474.
17. W.J. Lorenz, H.D. Hermann, N. Wüthrich, F. Hilbert, J. Electrochem. Soc. 121 (1974) 1167.
18. J. Horkans, B.D. Cahan, E. Yeager, J. Electrochem. Soc. 122 (1975) 1585.
19. S. Stucki, J. Electroanal. Chem. 78 (1977) 31.
20. A. Hamelin, A. Katayama, J.Electroanal. Chem. 117 (1981) 221.
21. S. Swathirajan, H. Mizota, S. Bruckenstein, J. Phys. Chem. 86 (1982) 2480.
22. A. Hamelin, J. Lipkowski, J. Electroanal. Chem. 171 (1984) 317.
23. K. Jüttner, Electrochim.Acta 29 (1984)1597.
24. O. Merloy, K. Kanazava, J.G. Gordon, D. Buttry, Langmuir 2 (1986) 697.
25. M.P. Green, K.J. Hanson, R. Carr, I. Lindau, J. Electrochem. Soc. 137 (1990) 3493.
26. B.E. Conway, J.S. Chacha, J. Electroanal. Chem. 287 (1990) 13.
27. A. Brunt, T. Rayment, S.J. O'Shea, M.E. Welland, Langmuir 12 (1996) 5942.
28. X. Zeng, S. Bruckenstein, J. Electrochem. Soc. 146 (1999) 2555.
29. M.P. Green, K.J. Hanson, D.A. Scherson, X. Xing, M. Richter, P.N. Ross, R. Carr, I. Lindau, J. Phys. Chem. 93 (1989) 2181.

30. M. Binggeli, D. Carnal, R. Nyffenegger, H. Siengenthaler, R. Christoph, H. Rohrer, J. Vac. Sci. Technol. B9 (1991) 1985.
31. C. Chen, N. Washburn, A. Gewirth, J. Phys. Chem. 97 (1993) 9754.
32. U.Schmidt, S. Vinzelberg, G. Staikov, Surf. Sci. 348 (1996) 261.
33. E. Herrero, L.J. Buller, H.D. Abruña, Chem. Rev.101 (2001)1897.
34. E. Kirowa-Eisner, Y. Bonfil, D. Tzur, E. Gileadi, J. Electroanal. Chem. 552 (2003) 171.
35. R. Vaidyanathan, J. L. Stickney, U. Happek Electrochim. Acta 49 (2004) 1321.
36. N.P. Osipovich, E.A. Streltsov, Elektrokhimiya 36 (2000) 5.
37. R.W. Andrews, D.C. Johnson, Anal. Chem. 47 (1975) 294.
38. T.A. Sorenson, T.E. Lister, B.M. Huang, J.L. Stickney, J. Electrochem. Soc. 146 (1999) 1019.
39. T.E. Lister, J.L. Stickney, D.E. Pnes, J. Whitten, Appl. Surf. Sci. 107 (1996) 153.
40. M. Alanyalioglu, U. Demir, C. Shannon, J. Electroanal. Chem. 561 (2004) 21.
41. E.A. Streltsov, S.K. Poznyak, N.P. Osipovich, J. Electroanal. Chem. 518 (2002) 103.
42. D.K. Ivanov, N.P. Osipovich, S.K. Poznyak, E.A. Streltsov, Surf. Sci. 532-535 (2003) 1092.
43. E.A. Streltsov, N.P. Osipovich, L.S. Ivashkevich, A.S. Lyakhov, Electrochim. Acta, 44 (1998) 407.
44. E.A. Streltsov, N.P. Osipovich, L.S. Ivashkevich, A.S. Lyakhov, V.V. Sviridov, Electrochim. Acta, 43 (1998) 869.
45. E.A. Streltsov, N.P. Osipovich, L.S. Ivashkevich, A.S. Lyakhov, Electrochim. Acta, 44 (1999) 2645.